may be normal modes that have decay times sufficiently long that the modes retain some level of disequilibrium even for the time scale of TPW considered here [hence, $\beta(t)$ would not have relaxed to β_∞]. We have found that the dominant, normal-mode contribution arises from the so-called M1 mode. The M1 mode arises from a deflection of the density discontinuity at a depth of 660 km between the upper and lower mantle. Thus, excitation of the mode requires that the discontinuity behaves nonadiabatically (that is, effectively as a chemical boundary) on the time scales we are considering. If this is not the case, then the mode would not be excited and the M1 contribution would vanish. As an example, the peak ~54 m signal in Fig. 4 (curve A) has a contribution of ~43 m from the elastic lithosphere and ~11 m from the M1 mode.

28. We define rotational colatitude as the angular distance of a site from the instantaneous north pole of rotation.
29. In the seismic stratigraphic analysis of short-term (third-order cycles and higher) sea-level change (*2*, *4*), North American and European sites dominate (Fig. 3C). The relative proximity of these sites suggests that they will experience similar TPW-induced sea-level trends. Thus, as has been suggested (*14*), it is unclear to what extent eustatic versus (TPW-induced) quadrant-localized signals contribute to the mean third-order sea-level trends.
30. See, for example, B. H. Hager, *J. Geophys. Res.* **89**, 6003 (1984); M. A. Richard and B. H. Hager, *ibid.*, p. 5987; M. Nakada and K. Lambeck, *Geophys. J. Int.* **96**, 497 (1989); Y. Ricard and B. Wuming, *ibid.* **105**, 561 (1991); J. X. Mitrovica, *J. Geophys. Res.* **101**, 555 (1996); A. M. Forte and J. X. Mitrovica, *Geophys. Res. Lett.* **23**, 1147 (1996).
31. The sensitivity to *LT* apparent in Fig. 5A follows from the arguments in (*27*). Furthermore, we have found that the contribution of the M1 mode to the sea-level signal (*27*) is sensitive to variations in upper mantle viscosity, and less sensitive to variations in lower mantle viscosity, for this range of Earth models; this explains the results in Fig. 5, B and C.
32. T. H. Jordan, *Rev. Geophys.* **13**, 1 (1975); S. P. Grand, *J. Geophys. Res.* **92**, 14065 (1987); A. M. Forte, A. M. Dziewonski, R. J. O'Connell, *Science* **268**, 386 (1995).
33. B. M. Steinberger and R. J. O'Connell, *Nature* **387**, 169 (1997).
34. Our sea-level predictions include the direct gravitational attraction and the loading effect of sea-level variations (*22*). The spatial geometry of these effects depends on the distribution of oceans, and therefore the sea-level trends we predict are more complicated than the simple illustrations in Fig. 3 imply.

35. We thank J. Wahr and two anonymous referees for their reviews of this report. We also thank D. Rowley for helpful comments. We are grateful for the ocean-continent geometry data provided by the PLATES Project of the Institute for Geophysics of the University of Texas at Austin. The work of J.X.M. was funded by Natural Sciences and Engineering Research Council of Canada and was supported by the Canadian Institute for Advanced Research (Earth Systems Evolution Program).

22 September 1997; accepted 2 December 1997

Catalytic Galactose Oxidase Models: Biomimetic Cu(II)–Phenoxyl-Radical Reactivity

Yadong Wang, Jennifer L. DuBois, Britt Hedman,* Keith O. Hodgson,* T. D. P. Stack*

Biomimetic functional models of the mononuclear copper enzyme galactose oxidase are presented that catalytically oxidize benzylic and allylic alcohols to aldehydes with O_2 under mild conditions. The mechanistic fidelity between the models and the natural system is pronounced. Modest structural mimicry proves sufficient to transfer an unusual ligand-based radical mechanism, previously unprecedented outside the protein matrix, to a simple chemical system.

An important goal of bioinorganic chemistry is the development of small inorganic complexes that not only reproduce structural and spectroscopic features, but also function in a manner similar to their natural counterparts. Despite much effort, faithful examples of catalytically functional models are rare, especially when O_2 is used as the oxidant (*1*). Presented here is a family of functional models of galactose oxidase (GOase) that catalytically oxidize benzylic and allylic alcohols to aldehydes with O_2 under mild conditions. The structural design of the models follows directly from the structure of the active site of the enzyme, and the ligand-based radical mechanism elucidated here parallels that proposed for the native system. Considering that a chemical precedent for this radical-based reaction outside a protein matrix has been lacking, the structural, spectroscopic, and mechanistic fidelity of these model complexes relative to the native system is striking.

GOase (*2*, *3*), a mononuclear copper enzyme, couples the oxidation of alcohols to aldehydes with the reduction of O_2 to H_2O_2 (Eq. 1) through an unusual Cu(II) phenoxyl-radical active species (*2*, *4*). Despite the importance of this organic transformation, there are few highly efficient, environmentally benign synthetic catalysts (*5*). The development of catalytically functional GOase models (*6*) allows this radical mechanism (*2*) to be probed more readily and also may lead to efficient catalysts.

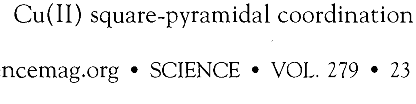

(1)

The crystal structure of GOase shows that the protein provides four ligands for the Cu(II) arranged in an unusual non-square–planar (nSP) coordination (Fig. 1A) (*7*): two tyrosine phenolates and two histidine imidazoles. A fifth exogenous H_2O ligand occupies an equatorial position in the Cu(II) square-pyramidal coordination. An interesting feature of this structure is a covalent thioether bond formed between a cysteine sulfur atom and an aromatic carbon of the equatorial phenolate ligand. It is this modified phenolate ligand that is thought to be oxidized to a radical, resulting in an electron paramagnetic resonance (EPR)–silent active form of the enzyme (*7*). The synthetic complexes reported here (Fig. 1B) possess a nSP Cu(II) N_2O_2 coordination geometry and appropriately positioned thioether substituents on the phenolate moieties (for BSI and BSP) (*8*). The x-ray crystal structure of one cupric complex, [Cu(II)BSI], confirms a nSP tetradentate ligation (Fig. 1C) (*9*), and EPR spectra of these Cu(II) complexes support a nSP geometry in solution as their $g_{\|}$ values are significantly larger than those of the related square-planar Cu(II) complexes (*10*).

These complexes have spectroscopic characteristics similar to those of GOase. With respect to reactivity, the most important is the formation of a room-temperature (RT) stable, EPR-silent species upon one-electron (1 e^-) oxidation of each Cu(II) complex (*11*). We recently reported that *o*,*p*-substitution of the phenolate ring in these Cu complexes is critical to stabilizing their oxidized EPR-silent form (*8*). Oxidation of the Cu(II) complexes requires a strong oxidant, because their potentials range from +0.80 to +1.1 V (versus a standard calomel electrode) (*12*). In this process, the ligand **L**, not the metal, is oxidized (Eq. 2); the copper center remains Cu(II), as established by the similarity in energy of features in Cu K-edge x-ray absorption spectra (XAS) for [Cu(II)BDB] and its 1 e^- oxidized form—in particular, the 1*s* → 3*d* pre-edge features at 8979 eV (Fig. 2) (*13*–*15*).

$$[\mathrm{Cu^{II}}\mathbf{L}] + \mathrm{NO^+(BF_4)^-} \rightarrow [\mathrm{Cu^{II}}\mathbf{L}(\mathrm{BF_4})]^{\cdot} + \mathrm{NO\ (g)} \qquad (2)$$

Y. Wang, J. L. DuBois, T. D. P. Stack, Department of Chemistry, Stanford University, Stanford, CA 94305-5080, USA.
B. Hedman, Stanford Synchrotron Radiation Laboratory, Stanford University, Stanford, CA 94309, USA.
K. O. Hodgson, Department of Chemistry, Stanford University, Stanford, CA 94305-5080, and Stanford Synchrotron Radiation Laboratory, Stanford University, Stanford, CA 94309, USA.

---

*To whom correspondence should be addressed. E-mail: hedman@ssrl.slac.stanford.edu; hodgson@ssrl.slac.stanford.edu; stack@leland.stanford.edu

However, the anticipated phenoxyl-radical absorption feature at ~400 nm is obscured by intense Schiff-base ligand absorption bands (*8*). Localization of the radical on a phenolate ring rather than the binaphthyl backbone is inferred from EPR parameters of the analogous, 1 e$^-$ oxidized Zn(II) complexes, [Zn(II)**L**]$^{+\bullet}$ (S = 1/2); the g values of [Zn(II)**L**]$^{+\bullet}$ complexes vary consistently with those of the isolated phenoxyl-radical fragments (*16, 17*).

An optical titration of the oxidized complex [Cu(II)BSP]$^{+\bullet}$ indicates a 1:1 anion affinity with methoxide (MeO$^-$), suggesting the formation of a five-coordinate complex, [Cu(II)BSP(OMe)]$^{\bullet}$. Pentadentate coordination of the Cu(II) center is supported by XAS data for the [Cu(II)BDB(OMe)]$^{\bullet}$ and [Cu(II)BDB(BF$_4$)]$^{\bullet}$ species (Fig. 3). A five-coordinate geometry is indicated for [Cu(II)BDB(BF$_4$)]$^{\bullet}$ by the similarity of the absorption edge shape relative to those of crystallographically characterized five-coordinate Cu(II) complexes (*13, 18*), and the extended x-ray absorption fine-structure (EXAFS) analysis shows that a fluoride of BF$_4^-$ is bound at 2.67 Å in addition to the N$_2$O$_2$ atoms of the ligand (*19*). A comparison of the four N/O ligating distances in [Cu(II)BDB] and [Cu(II)BDB(BF$_4$)]$^{\bullet}$ shows that the average Cu-O(N) bond distances increase only slightly upon oxidation, similar to the changes observed for GOase (*20*) and other small metal complexes with an attached phenoxyl radical (*21*). A more dramatic rearrangement of the BDB ligand occurs by ligation of MeO$^-$, a significantly stronger ligand than BF$_4^-$. The structure of this methoxide complex should be similar to the substrate-bound intermediate in the proposed catalytic cycle (see below). Pentadentate coordination is consistent with both the XAS edge shape and the EXAFS model. The equatorial ligands are likely the two O(N) at a short distance of 1.93 Å (possibly one MeO$^-$ and one phenolate) and the two N(O) at an average distance of 2.12 Å. The limited ligand flexibility would require the remaining phenolate to be bound in an axial position, consistent with the long 2.54 Å Cu-O(N) distance observed.

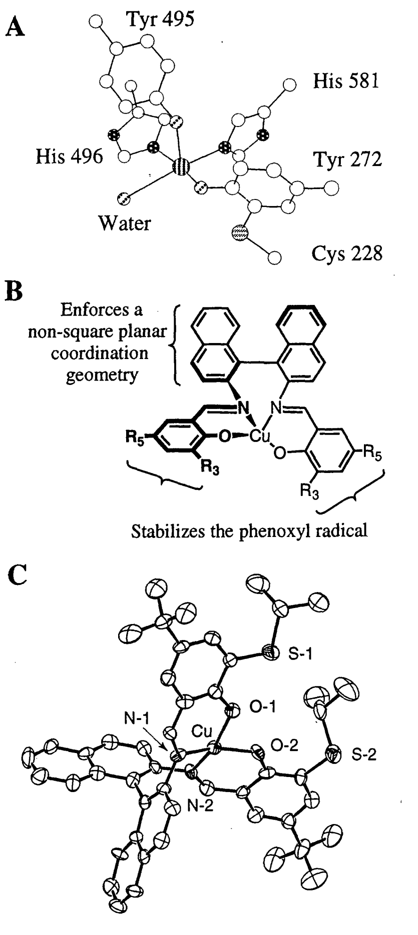

Fig. 1. (**A**) Copper active site of GOase at pH 7.0 (*7*). (**B**) Complex nomenclature, labeling, and structure. For [Cu(II)BSP], R$_3$ is SPh and R$_5$ is Bu^t; for [Cu(II)BSI], R$_3$ is SPr^i and R$_5$ is Bu^t; for [Cu^{II}BDB], both R$_3$ and R$_5$ are Bu^t; for [Cu^{II}BBR], both R$_3$ and R$_5$ are Br. (**C**) ORTEP representation (50% thermal ellipsoids) of the x-ray crystal structure of [Cu(II)BSI]. Selected distances (in angstroms) are as follows: Cu to O-1, 1.900; Cu to O-2, 1.894; Cu to N-1, 1.959; Cu to N-2, 1.982; dihedral angle between two planes defined by (Cu, N-1, O-1) and (Cu, N-2, O-2), 30°.

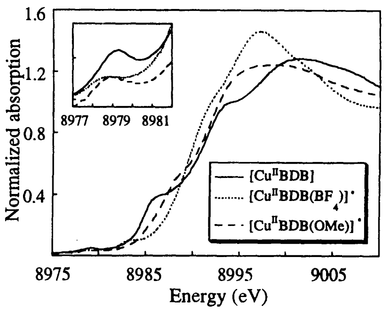

Fig. 2. The Cu K-edge XAS of [Cu(II)BDB], [Cu(II)BDB(BF$_4$)]$^{\bullet}$, and [Cu(II)BDB(OMe)]$^{\bullet}$. Inset amplifies the pre-edge features (1*s* → 3*d* transition) at ~8979 eV, indicative of a Cu(II) in all three complexes (*14*).

With phenylmethoxide (PhCH$_2$O$^-$) ligated, the complex converts stoichiometrically at RT to benzaldehyde and a Cu(I) complex under anaerobic conditions (*8*). Under 1 atm of O$_2$, neat benzylic and allylic alcohols are catalytically converted to their respective aldehydes or ketones (Table 1). The reaction requires only a catalytic amount of base (*22*), runs at RT, and can achieve >1000 turnovers (*23*). Further oxidation of the aldehyde products is not observed. The catalytic reaction also occurs, although much less efficiently, in acetonitrile solutions (Table 1).

A mechanistic scheme for this reaction is proposed (Fig. 4) from studies with the most efficient catalyst and substrate, [CuBSP] and benzyl alcohol (PhCH$_2$OH), respectively. The catalytic reaction may be started with the catalyst in three different forms (Table 1 and Fig. 5): the aerobically isolated form {[Cu(II)BSP]}, the preoxidized form {[Cu(II)BSP(BF$_4$)]$^{\bullet}$},

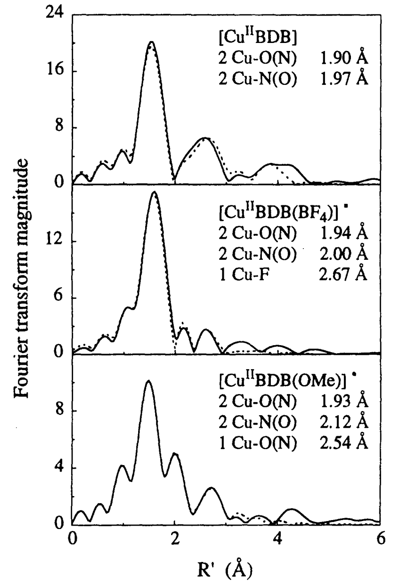

Fig. 3. Fourier transforms of the EXAFS spectra (solid line) of [Cu(II)BDB], [Cu(II)BDB-(BF$_4$)]$^{\bullet}$, and [Cu(II)BDB(OMe)]$^{\bullet}$ along with theoretical fits (dotted line) (*15*) and metrical-fit results for the models.

Table 1. Turnovers achieved for reactions at 1 atm of O$_2$ and 295 K after 20 hours.

Catalyst	Neat substrate*		Acetonitrile solution (1.5 M)		
	Benzyl alcohol†	1-Phenyl ethanol‡	Benzyl alcohol§	1-Phenyl ethanol‖	Cinnamyl alcohol‖
[Cu(II)BSP(BF$_4$)]$^{\bullet}$	1300				
[Cu(II)BSP]	1300¶	60	400	30	40
[Cu(I)BSP]$^-$	900				
[Cu(II)BDB]	200¶	30	40	30	30

*No reactivity was achieved for 1-octanol or cyclohexanol as neat substrates with [Cu(II)BSP] or [Cu(II) BDB]. †0.01% catalyst and 2% base. ‡0.05% catalyst and 0.3% base. §0.005% catalyst and 0.2% base. ‖0.05% catalyst and 0.5% base. ¶For 0.06% catalyst and 1.2% base, turnovers are 300 for [Cu(II)BSP] and 50 for [Cu(II)BDB]. For base, see (*22*).

and the prereduced form {[Cu(I)BSP]$^-$}. Under identical reaction conditions, all three forms generate an approximately equal number of turnovers. However, the initial reaction rate is significantly slower for [Cu(II)BSP] than for the other two forms (Fig. 5). Initially, the most reactive form is [Cu(II)BSP(BF_4)]$^{\bullet}$, and optical titrations indicate that ligand exchange of BF_4^- by alkoxide is rapid. Thus, [Cu(II)BSP (OCH_2Ph)]$^{\bullet}$ is a kinetically competent intermediate for all three forms of the catalyst (Fig. 4). Under pseudo–first order conditions of excess substrate $PhCH_2O^-$ and $PhCD_2O^-$, a competitive kinetic-isotope effect (KIE) of 5.3 is found when the reaction is started with [Cu(II)BSP]. This result strongly implicates that cleavage of the benzylic C^{α}-H bond is involved in the rate-determining step (RDS) of the catalytic cycle. A similar KIE value of 7.7 is found for GOase (*24*). Given the radical character of the phenoxyl O atom and its proximity to the benzylic H atoms of the substrate (Fig. 4), a H-atom abstraction mechanism is reasonable. Slight variations of the reaction rate with various *p*-substituted benzylic alcohols give a Hammett ρ value of −0.14 (*17*), consistent with this mechanism. The lack of observed reactivity of primary and secondary alkyl alcohols at RT with these catalysts (Table 1) is consistent with their greater Cα-H bond strengths compared with benzylic or allylic alcohols (>7 kcal/mol) (*25*). Similar reactivity trends are found for GOase, which oxidizes primary alkyl alcohols at rates >10^3 times slower than benzylic substrates (*26*).

The similar initial reaction rates of [Cu(II)BSP(BF_4)]$^{\bullet}$ and [Cu(I)BSP]$^-$ in conjunction with the O_2 sensitivity of [Cu(I)BSP]$^-$ suggest that O_2 oxidizes [Cu(I)BSP]$^-$ by 2 e$^-$ to form a hydroperoxide species, [Cu(II)BSP (OOH)]$^{\bullet}$. This species subsequently undergoes facile ligand exchange of the peroxide with $PhCH_2O^-$ to generate the active form [Cu(II)BSP(OCH_2Ph)]$^{\bullet}$ (*27*). Given the greater acidity of H_2O_2 relative to $PhCH_2OH$ (*28*), the final equilibrium step of the cycle will be favorable only under low H_2O_2 or high alkoxide concentrations, or both. Indeed, added H_2O_2 inhibits this catalytic reaction (*29*), and higher alkoxide concentrations enhance the initial reaction rates.

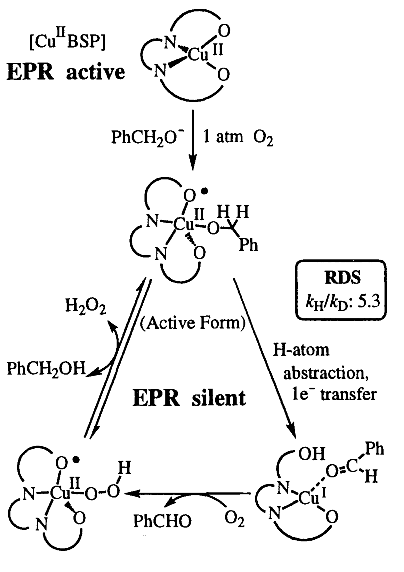

Fig. 4. Proposed catalytic cycle for model complex [CuBSP].

Although spectroscopic evidence for [Cu(II)BSP(OOH)]$^{\bullet}$ is currently lacking, its presence is inferred from the measured 1:1 ratio of O_2 uptake to aldehyde product at early stages of the reaction (*17, 30*). Additional evidence for this 2 e$^-$ oxidation of [Cu(I)BSP]$^-$ by O_2 is provided by the EPR silence of the major reaction product (~90%) that results from injection of (Bu_4N)[Cu(I)BSP] (*17*) into a saturated O_2 solution (*31*); only ~10% is converted to an EPR-active Cu(II) complex. This 2 e$^-$ oxidation is unexpected, as the aerobically stable form is [Cu(II)BSP]. However, the intermediacy of the aerobically isolated form, [Cu(II)BSP], in this reaction is excluded by its significantly slower initial catalytic reactivity relative to [Cu(I)BSP]$^-$ (Fig. 5).

A final issue concerns the slow initial catalytic reactivity of [Cu(II)BSP]. The catalytic reactivity correlates with a loss of Cu(II) EPR intensity, suggesting the 1 e$^-$ oxidized complex as the active form. Oxidization of [Cu(II)BSP] by O_2 does not occur in alcoholic media as assessed by Cu(II) EPR spectroscopy. However, the addition of alkoxide and O_2 does result in a slight diminution of the EPR intensity after 30 min (~5%). The equilibrium constant of MeO^- binding to [Cu(II)BSP] to form [Cu(II) BSP(OMe)]$^-$ is small, as indicated by optical titrations. However, the binding of MeO^- significantly attenuates the oxidation potential of the resulting complex, making it potentially susceptible to oxidation by O_2. An estimate of this potential is obtained from the irreversible reduction potential of [Cu(II)BSP(OMe)]$^{\bullet}$ (~0.00 V), which may be independently synthesized. The slow initial catalytic reactivity observed using [Cu(II)BSP] (Fig. 5) is consistent with its slow conversion to [Cu(II)BSP]$^{+\bullet}$.

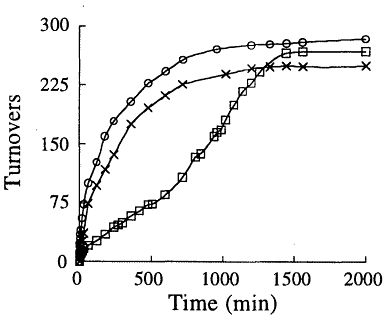

Fig. 5. Comparison of reaction rate with different starting catalysts. Open circles, [Cu(II)BSP]$^{+\bullet}$; crosses, [Cu(I)BSP]$^-$; open squares, [Cu(II)BSP]. Benzyl alcohol with (v/v) 15% CH_2Cl_2, 10% MeCN, 0.01% catalyst, 0.2% base, 1 atm of O_2 at RT.

The transfer of the chemical reactivity of an enzyme into a simple chemical system requires preclusion of deleterious, bimolecular side reactions that the native system avoids by isolating the active site in a protein matrix; in this particular case, complete *o,p*-substitution of the phenolate rings is necessary, which likely prevents ligand-radical coupling (*8*). These modifications result in complexes that exhibit oxidase reactivity strikingly similar to GOase (*2, 32*). In both cases, the proposed active form is a five-coordinate, Cu(II) phenoxyl-radical species with alkoxide substrate bound, the RDS involves Cα-H bond scission of the substrate, O_2 is used as a 2 e$^-$ oxidant, and one equivalent each of H_2O_2 and aldehyde are produced in each cycle. Additionally, the reaction is inhibited by H_2O_2 (*29, 33*).

These similarities likely result from integration of key structural attributes of the active site of GOase into the synthetic complexes. The enforced nSP coordination geometry, although not preferred by a Cu(II) ion, is sufficient to form a stable four-coordinate Cu(II) complex. Oxidation by 1 e$^-$ yields a cationic complex that, not unexpectedly, binds an additional exogenous anionic ligand (substrate). The flexibility of these ligands to accommodate both five- and four-coordinate geometries without the intermediacy of a square-planar complex is potentially important for stabilization of the active form (*34*). This ligand flexibility is also potentially important in the facile oxidation of a Cu(I) complex directly to [Cu(II)**L**]$^{+\bullet}$ by O_2 rather than to two equivalents of [Cu(II)**L**]. This biomimetic success along with the recent wealth of new structural information on metalloproteins promises that other unusual biological catalytic reactivities may be transferred to small chemical systems.

REFERENCES AND NOTES

1. J. T. Groves and Y.-Z. Han, in *Cytochrome P-450, Structure, Mechanism and Biochemistry*, P. R. Ortiz de Montellano, Ed. (Plenum Press, New York, ed. 2, 1995), pp. 3–48 and references therein; M. Réglier, C. Jorand, B. Waegell, *J. Chem. Soc. Chem. Commun.* **1990**, 1752 (1990); W. O. Koch and H. J. Krüger, *Angew. Chem. Int. Ed. Engl.* **34**, 2671 (1996).
2. M. M. Whittaker and J. W. Whittaker, *Biophys. J.* **64**, 762 (1993).
3. J. P. Klinman, *Chem. Rev.* **96**, 2541 (1996).

4. M. M. Whittaker, V. L. DeVito, S. A. Asher, J. W. Whittaker, *J. Biol. Chem.* **264**, 7104 (1989).
5. I. E. Markó *et al.*, *Science* **274**, 2044 (1996); C. Zondervan, R. Hage, B. L. Feringa, *Chem. Commun.* **1997**, 419 (1997).
6. For GOase model studies, see J. A. Halfen *et al.* [*J. Am. Chem. Soc.* **119**, 8217 (1997)] and references therein.
7. N. Ito *et al.*, *Nature* **350**, 87 (1991); N. Ito *et al.*, *J. Mol. Biol.* **238**, 794 (1994).
8. Y. Wang and T. D. P. Stack, *J. Am. Chem. Soc.* **118**, 13097 (1996). These model complexes are shown to catalytically convert benzyl alcohol to benzaldehyde with a strong organic-radical oxidant.
9. Crystal data for [Cu(II)BSI]: a brownish green crystal from tetrahydrofuran layered with pentane; triclinic $P\bar{1}$ (2), a = 10.4865(9) Å, b = 15.996(1) Å, c = 17.986(2) Å, α = 69.347(1)°, β = 88.254(1)°, γ = 81.377(1)°, V = 2790.2(4) Å^3, Z = 2; 3579 reflections [$I > 4\sigma(I)$, 4.5° $< 2\theta <$ 45.4°], $R(R_w)$ = 8.7(9.7).
10. The $g_{\parallel}$ value for [Cu(II)BDB] is 2.231, whereas that for its square-planar analog (a cyclohexyl-1,2-diimine backbone) is smaller at 2.195 [E. I. Solomon, *Comm. Inorg. Chem.* **III**, 227 (1984)].
11. The stoichiometry has been determined by both EPR (77 K) and optical titrations (RT).
12. The Cu(II) complexes are oxidized either by tris(4-bromophenyl)aminium hexachloroantimonate, [(TPA$^+$)-(SbCl$_6^-$)], or nitrosonium tetrafluoroborate [(NO)$^+$-(BF$_4$)$^-$].
13. L. S. Kau *et al.*, *J. Am. Chem. Soc.* **109**, 6433 (1987).
14. J. L. DuBois *et al.*, *ibid.* **119**, 8578 (1997).
15. The Cu K-edge XAS spectra were obtained at Stanford Synchrotron Radiation Laboratory (SSRL): Si(220) double-crystal monochromator, detuned 50% at 9868 eV, transmission on solids in a matrix of boron nitride, internal Cu foil calibration, first Cu foil edge inflection point assigned to 8980.3 eV. Theoretical EXAFS signals $\chi(k)$ are calculated and fit to the data by using the GNXAS suite of programs [A. Filipponi, A. Di Cicco, T. A. Tyson, C. R. Natoli, *Solid State Commun.* **78**, 265 (1991); T. E. Westre *et al.*, *J. Am. Chem. Soc.* **117**, 1566 (1995)]. EXAFS data to k = 13 Å^{-1} yielded first coordination shells easily resolvable into two or three average ligand distances per complex. The [Cu (II)BDB] distances agree very well with x-ray crystallographic data for [Cu(II)BSI] (Fig. 1 legend).
16. Larger g values observed for the Br and S substituted ligands result from the larger spin-orbit couplings of heavier elements. The g values for the Zn analogs and their corresponding phenoxyl radicals are as follows: [Zn(II)BSP]$^{+\bullet}$, 2.0060; 2-thiomethyl-4-methylphenoxyl, 2.0059; [Zn(II)BDB]$^{+\bullet}$, 2.0045; 2,4-di-*t*-butylphenoxyl, 2.0045; [Zn(II)BBr]$^{+\bullet}$, 2.0057; 2,4-dibromophenoxyl, 2.0061. See Fig. 1 legend for nomenclature. Stable Zn phenoxyl-radical species have been reported [A. Sokolowski *et al.*, *J. Am. Chem. Soc.* **119**, 8889 (1997)].
17. See supporting information (available upon request or through the *Science* Online Web site at www.sciencemag.org) for synthetic details, spectroscopic data for all new compounds, and x-ray crystal structural information.
18. This study concerns the coordination geometry of Ni complexes [G. J. Colpas *et al.*, *Inorg. Chem.* **30**, 920 (1991)].
19. Fluoride abstraction from counterions by Cu(II) has been documented [S. C. Lee and R. H. Holm, *Inorg. Chem.* **32**, 4745 (1993)]. A BF$_4^-$ rather than a F$^-$ ligand is assumed from the bond length [Cambridge Structural Database; 19 examples of Cu(II)-FBF$_3$: 2.39 to 2.85 Å, 26 examples of Cu(II)-F: 1.85 to 2.23 Å].
20. P. F. Knowles *et al.*, *Inorg. Chem.* **34**, 3895 (1995).
21. Structural characterization of a phenoxyl-radical chromium complex shows only a +0.02 Å increase in the Cr-OPh bond distance relative to the phenoxy ligand [A. Sokolowski *et al.*, *J. Chem. Soc. Chem. Commun.* **1996**, 1671 (1996)].
22. Both lithium and sodium alkoxides have been suitable.
23. Two monomeric Cu complexes have been reported to catalyze oxidation of alcohols to aldehydes with O$_2$ as the oxidant with either a stoichiometric or an excess amount of base, respectively [N. Kitajima, K. Whang, Y. Moro-oka, A. Uchida, Y. Sasada, *J. Chem. Soc. Chem. Commun.* **1986**, 1504 (1986); J. T. Groves and K.-T. Park, in *Studies in Organic Chemistry: The Role of Oxygen in Chemistry and Biochemistry*, W. Ando and Y. Moro-oka, Eds. (Elsevier, Amsterdam, 1988), vol. 33, pp. 541–548].
24. A. Maradufu, G. M. Cree, A. S. Perlin, *Can. J. Chem.* **49**, 3429 (1971).
25. D. F. McMillen and D. M. Golden, *Annu. Rev. Phys. Chem.* **33**, 493 (1982).
26. G. A. Hamilton, J. De Jersey, P. K. Adolf, in *Oxidases and Related Redox Systems*. T. E. King, H. S. Mason, M. Morrison, Eds. (University Park Press, Baltimore, MD, 1973), vol. 1, pp. 103–124.
27. Two rapid, sequential, 1 e$^-$ transfers through the intermediacy of a superoxide-Cu(II) species will be considered mechanistically indistinguishable from a concerted 2 e$^-$ transfer.
28. The aqueous pK_a values for H$_2$O$_2$ and PhCH$_2$OH are about 12 and 16, respectively. Although the pK_a values in PhCH$_2$OH will certainly be much higher, the ratio of the values should remain effectively constant.
29. The reaction rate dramatically decreases as the reaction proceeds, probably because of H$_2$O$_2$ inhibition. Addition of a 100-fold excess of 1,4-diazabicyclo[2,2,2]octane H$_2$O$_2$ [P. G. Cookson, A. G. Davies, N. Fazal, *J. Organometallic Chem.* **99**, C31 (1975)] to the reaction mixture inhibits the catalysis.
30. In the later stages of the reaction, the O$_2$:benzaldehyde ratio slowly increases to ~2:1, consistent with disproportionation of H$_2$O$_2$ to water and O$_2$, a reaction known to be catalyzed by Cu(II) complexes. Positive qualitative tests for H$_2$O$_2$ with KI containing starch and an aqueous Ti(IV) reagent [W. C. Wolfe, *Anal. Chem.* **34**, 1328 (1962)] are also observed.
31. Excess O$_2$: 0.1 ml of a 1.0 mM CH$_2$Cl$_2$ solution of [Cu(I)BSP]$^-$ at RT was injected directly into 0.9 ml of CH$_2$Cl$_2$ that was presaturated with 1 atm of O$_2$ ([O$_2$] = 3.8 mM) [K. D. Karlin *et al.*, *J. Am. Chem. Soc.* **116**, 1324 (1994)].
32. R. M. Wachter and B. P. Branchaud, *ibid.* **118**, 2782 (1996).
33. G. A. Hamilton *et al.*, *ibid.* **100**, 1899 (1978).
34. Square-planar Schiff-base Cu(II) complexes are found to be oxidized to reasonably stable EPR-silent [Cu(II)**L**]$^{+\bullet}$ species. However, these complexes do not oxidize alcohols.
35. Supported by grants from NIH [GM50730 (T.D.P.S.)], NIH [RR-01209 and NSF CHE-9423181 (K.O.H.)], and a Shell Faculty Career Initiation Award (T.D.P.S.). We thank the UCSF Mass Spectrometry Facility. SSRL operations are funded by the Department of Energy (DOE), Office of Basic Energy Sciences. The Biotechnology Program is supported by the NIH, National Center for Research Resources, Biomedical Technology Program. Further support is provided by the DOE, Office of Biological and Environmental Research.

6 October 1997; accepted 5 December 1997

Bimetallic System for Nitrogen Fixation: Ruthenium-Assisted Protonation of Coordinated N_2 on Tungsten with H_2

Yoshiaki Nishibayashi, Shotaro Iwai, Masanobu Hidai*

Treatment of the tungsten dinitrogen complex *cis*-[W(N$_2$)$_2$(PMe$_2$Ph)$_4$] (Me = methyl, Ph = phenyl) with an equilibrium mixture of [RuCl(dppp)$_2$]X and *trans*-[RuCl(η^2-H$_2$)(dppp)$_2$]X [X = BF$_4$, PF$_6$, or OSO$_2$CF$_3$; dppp = 1,3-bis(diphenylphosphino)propane] under 1 atmosphere of dihydrogen at 55 degrees Celsius for 24 hours gave NH$_3$ in moderate yield. The same reaction in the presence of acetone produced acetone azine in high yield. None of these reactions proceeded in the absence of dihydrogen.

Dinitrogen has been regarded as one of the most inert molecules under normal laboratory conditions. Industrially, organonitrogen compounds fundamentally depend for their nitrogen source on NH$_3$ produced by the energy-consuming Haber-Bosch process, where extremely drastic reaction conditions are required in order to activate N$_2$ (*1*). The development of chemical processes that enable direct transformation of N$_2$ into compounds such as NH$_3$ and organonitrogen compounds under mild conditions is an important goal.

Studies of the reactivities of coordinated N$_2$ in complexes of the type M(N$_2$)$_2$(L)$_4$ (M = Mo or W; L = phosphine) (*2*)—the first of which is *trans*-[Mo(N$_2$)$_2$(dppe)$_2$] [dppe = 1,2-bis(diphenylphosphino)ethane], prepared by our group in 1969 (*3*)—have shown that the ligating N$_2$ can be transformed into NH$_3$ or hydrazine by treatment with inorganic acids such as H$_2$SO$_4$ and HCl (*4*). A detailed mechanism for the formation of nitrogen hydrides has been proposed on the basis of the reactivities of isolable intermediate complexes such as hydrazido(2-) complexes (*4*). However, H$_2$ could not be used for the synthesis of nitrogen hydrides because H$_2$ replaced the ligating N$_2$ in the complexes to form MH$_4$(L)$_4$ without formation of the N–H bond (*5*). Previously, metal carbonyl hydrides such as HCo(CO)$_4$ were used for the N–H bond formation of the coordinated N$_2$ (*6*). Recently, Morris *et al.* tried to use an acidic H$_2$ complex [CpRu(dtfpe)H$_2$]BF$_4$ {Cp = η^5-C$_5$H$_5$; dtfpe = 1,2-bis[bis(*p*-trifluoromethylphenyl)phosphino]ethane} with pK_a = 4.3 (K_a is the acid

---

Department of Chemistry and Biotechnology, Graduate School of Engineering, The University of Tokyo, 7-3-1 Hongo, Bunkyo-ku, Tokyo 113, Japan.

*To whom correspondence should be addressed.